JOURNAL OF APPLIED ELECTROCHEMISTRY 10 (1980) 495–504

Evaluation of zinc sulphate electrolytes containing certain impurities and additives by cyclic voltammetry

D. R. FOSNACHT

Inland Steel Company, East Chicago, Indiana, USA

T. J. O'KEEFE

Department of Metallurgical Engineering, University of Missouri-Rolla, Rolla, Missouri, USA

Received 17 August 1979

The polarization characteristics of acid zinc sulphate electrolytes containing various amounts of germanium and cobalt were examined by cyclic voltammetry. The effects of zinc and acid concentration, temperature, and surface preparation were also investigated. Small concentrations of impurities are shown to cause measurable changes in polarization behaviour. Levels as low as 0.02 $mg l^{-1}$ Ge and 0.1 $mg l^{-1}$ Co can be detected using this technique. The actual mechanism of impurity behaviour is more clearly delineated using this technique and evaluation of the data from these tests indicate that germanium and cobalt form local galvanic cells. The results of these short-term tests are shown to correlate with classical long-term efficiency tests. The deposit morphologies obtained for short-time cathodic cycles were also studied using scanning electron microscopy.

1. Introduction

The presence of impurities in the electrolyte is a major problem for the zinc electrowinning industry. Decreases in zinc current efficiency and changes in deposit morphology and cathodic polarization occur for electrolytes containing small concentrations of impurities. Levels as low as parts per billion for antimony, germanium, and arsenic and parts per million for cobalt are reported to greatly influence the cathodic deposition of zinc [1–19].

Impurity behaviour is not well understood and many questions remain regarding the acceptable limits of impurities for efficient operation of a zinc electrolysis circuit. Characterization of the electrolyte is very important and extensive analyses are conducted to determine the levels of impurities in the electrolyte. Chemical analyses have always served as the primary means of evaluating the quality of the electrolyte. Unfortunately, not only the absolute magnitude of the various impurities, but also the synergistic interactions among them ultimately determine the quality of deposits from the solution. Thus, a rapid electrochemical evaluation test to complement existing analyses would be desirable. A promising development in this area is the application of cyclic voltammetry to evaluate zinc-bearing electrolytes. Recent investigations have shown that glue additions to antimony-containing zinc electrolytes can be optimized using this technique [2, 4, 6]. Low levels of antimony and glue were found to cause measurable changes in cathodic polarization. The application of this technique to electrolytes containing nickel impurities indicated that nickel levels as low as 0.05 $mg l^{-1}$ could be detected [20]. The mechanism of nickel interaction was also evaluated using this technique.

In the present study, scanning electron microscopy and cyclic voltammetry were used in an attempt to characterize the effects of cobalt and germanium on cathodic polarization and zinc deposition. The techniques were used to gain some insight into the mechanism of impurity interaction at the cathode and to develop a practical test procedure which could be applied to cathodic zinc processes.

0021–891X/80/040495–10$03.00/0

2. Experimental

2.1. *Solution preparation*

A stock solution of neutral (pH = 4.0 − 4.5) purified zinc sulphate solution was prepared by using high-purity French process zinc oxide powder and reagent grade sulphuric acid. The zinc sulphate was purified by adding 0.1–0.2 ml l^{-1} 0.1 N $KMnO_4$; heating to near the boiling point with vigorous stirring; settling of the precipitates for 30 min at 80–85° C and then filtering. The filtrate was purified by adding 2 g l^{-1} zinc dust; heating to the boiling point with stirring for 30–45 min and then filtering to remove excess zinc dust. An analysis of the neutral purified solution appears in Table 1. Electrolytes of varying zinc contents were prepared using this solution.

Cobalt solution was prepared by dissolving cobaltous sulphate in distilled water to a concentration of 800 mg l^{-1}. A stock solution of germanium (10 mg l^{-1}) was prepared by dissolving the germanium in dilute sulphuric acid after GeO_2 was fused with Na_2CO_3 and K_2CO_3. All the stock solutions were analysed by atomic absorption analysis. The solutions were sorted in plastic bottles and analysed periodically.

Test solutions were prepared by taking the required amount of neutral purified solution, reagent grade sulphuric acid, impurity solution, and glue and placing them in a 500 ml volumetric flask. The volume was adjusted to 500 ml by adding distilled water.

Table 1. Analysis of neutral purified solution (mg l^{-1})

	Prepared
Zn	130 000
Mn	0.1
Cd	1.3
Sb	0.01
As	0.04
Ge	0.002
Co	0.1
Ni	0.05
Fe	0.4
Cu	0.08
F^-	0.1
Cl^-	1.0

2.2. *Cyclic voltammetry*

The cyclic voltammetry experiments were conducted in a Pyrex 'H' cell employing an Al working electrode (area 1 cm^2), a Pt counter electrode, and a mercurous sulphate reference electrode. A constant temperature water bath was used to maintain the desired temperature. A Petrolite Potentiodyne Analyser (Model M-4100) was used to record the cyclic voltammograms. The polarization behaviour was recorded as a log current density versus potential plot. The experimental apparatus has been described previously [4].

The working electrodes were prepared by wet polishing on 600 grit paper. The electrodes were washed in an ultrasonic cleaner after polishing and then rinsed with distilled water and dried with hot air. The electrodes were then placed in the 'H' cell and allowed to come to the test temperature. Tests were also conducted on electrodes which were wheel polished using 0.05 μm γ-alumina. The cleaning and drying procedures were the same as described previously.

After reaching the test temperature, a voltammogram was obtained by varying the potential from − 0.600 V versus SHE to a more cathodic potential where the total current was 50 mA cm^{-2}. At this point, the process was reversed and driven to the original starting potential. Various scan rates were tried, but 0.5 mV s^{-1} gave the most consistent results and was employed for the bulk of the studies. The factors studied were temperature, surface preparation, and additive, acid, and zinc concentrations.

In addition to the transient studies, tests were performed using constant potentials to determine the stability of the deposited zinc under various conditions. The morphologies of the zinc deposits were obtained using scanning electron microscopy.

3. Results and discussion

In order to gain a better understanding of the interpretation of the voltammograms, a review of the reactions thought to be occurring at the characteristic portions of a typical curve for an unadulterated electrolyte is given. Other reactions are initiated as additives or impurities are put into solution, and these must be considered when evaluating the electrolyte. The more important of

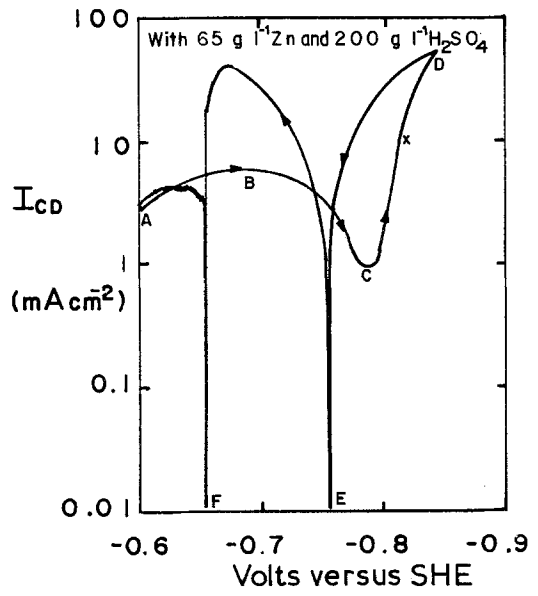

Fig. 1. Voltammogram for no-addition electrolyte. $T = 45°$ C; scan rate = 0.5 mV s^{-1}.

these are the reduction of the impurity ion and subsequent hydrogen evolution from the foreign metal.

3.1. *Voltammograms for no-addition electrolytes*

For an electrolyte containing 65 g l^{-1} Zn and 200 g l^{-1} H_2SO_4 and a 45° C temperature, a voltammogram of the type shown in Fig. 1 is obtained. From point A to point C (− 0.782 V versus SHE), only hydrogen evolution on the aluminium substrate occurs. At potentials more negative than point C (the zinc deposition potential), both hydrogen evolution and zinc deposition occur on the aluminium substrate. At point D, the scan direction is reversed and the potential is changed in an anodic direction.

Stability tests were conducted on the electrolyte to determine the potential where the zinc becomes anodically active. It was found that the zinc becomes unstable at a potential roughly 20 mV more negative than point E (or − 0.781 V versus SHE). When the potential was held at this value, the zinc completely dissolved after 20 min. At potentials more negative than this point, the current reaches a steady state value and zinc can be detected on the electrode surface. At point E (− 0.761 V versus SHE), the net current becomes anodic and stays anodic until point F is reached. The elimination of the zinc from the electrode causes the anodic current to drop and after point F the current again becomes cathodic and only hydrogen discharge occurs. From E to F, the zinc dissolution current is higher than the hydrogen reduction current and the net current is therefore anodic. Hysteresis of the curve exists because of the greater overpotential required to nucleate and grow zinc on the aluminium substrate. Zinc deposition on zinc requires less activation overpotential, so the current is higher on the reverse sweep due to the presence of a substantial amount of crystalline zinc.

A separate test was conducted to determine the reasons for the decrease in hydrogen discharge from B to C. The results, shown in Fig. 2, indicate that the hydrogen current continually increases for solutions containing only sulphuric acid. When 1 M $MgSO_4$ is added, some polarization occurs. The general shape of the curves in both cases is, however, quite similar. The decreased current is probably due to physical adsorption of the Mg^{2+} ions in the double layer.

The addition of zinc ions to the acid solution

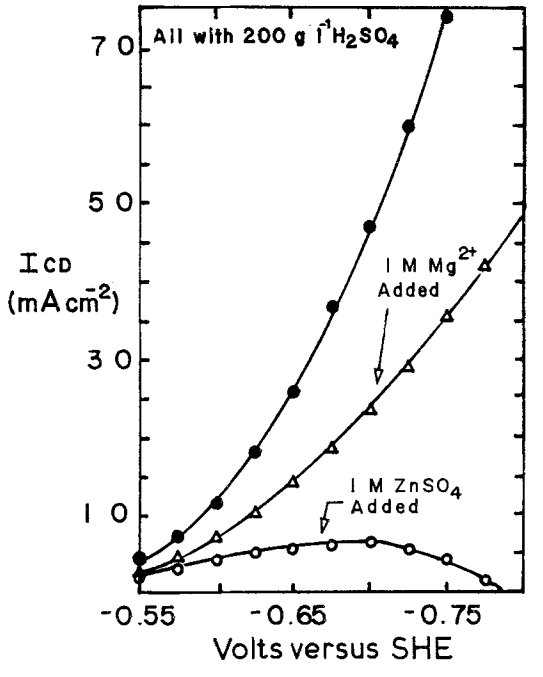

Fig. 2. Hydrogen current density versus electrode potential for electrolytes containing 200 g l^{-1} H_2SO_4 and the indicated additions. $T = 45°$ C; scan rate = 0.5 mV s^{-1}.

causes considerably greater polarization and a change in the shape of the curve as well. Initially, the hydrogen current increases slightly when the potential becomes more negative, but a current maximum is reached. Up to this point, the zinc ions may act similarly to the magnesium ions, but beyond this point they dramatically suppress hydrogen current. The large decrease in hydrogen current appears to be due to the specific adsorption of zinc ions or other species formed on the aluminium substrate that alter the hydrogen discharge reaction [21–23]. Zinc ion adsorption is reported to hinder the discharge of cobalt, nickel and iron in a similar fashion [22, 23], and appears to be one of the dominating factors in zinc electrowinning.

3.2. *Voltammograms for electrolytes containing germanium or cobalt additions*

The presence of low levels of Co and Ge impurities causes changes in the zinc polarization curve as illustrated in Figs. 3 and 4. Levels as low as 0.08 mg l^{-1} germanium and 1 mg l^{-1} cobalt cause measurable changes in polarization for electrolytes containing 65 g l^{-1} Zn and 200 g l^{-1} H_2SO_4.

At low levels of these impurities, a small inflection appears in the basic curve at point i. Upon increasing the impurity content, this changes to a plateau and finally to a hump or peak at point ai. The sequence of changes which occur are shown in Fig. 4. The value of the current density at point ai (subsequently called the peak current density) is found to be proportional to the amount of impurities in the electrolyte. Fig. 5 illustrates the trend of this peak current density with increasing cobalt content at 45 and 55° C. Increasing the

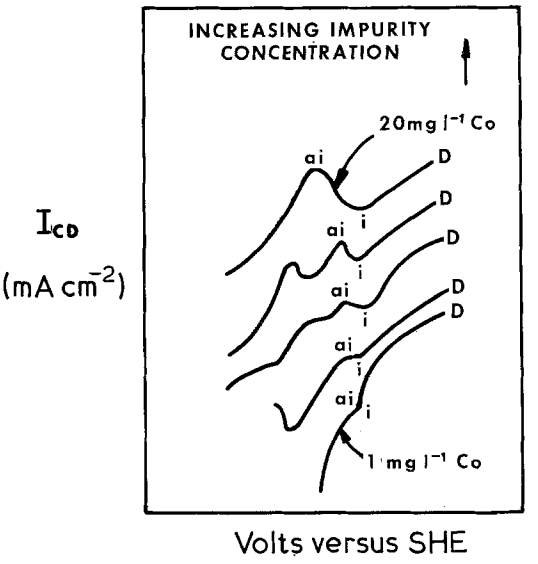

Fig. 4. Sequence of changes that occur at points i and ai as the impurity concentration increases for electrolytes containing germanium or cobalt additions.

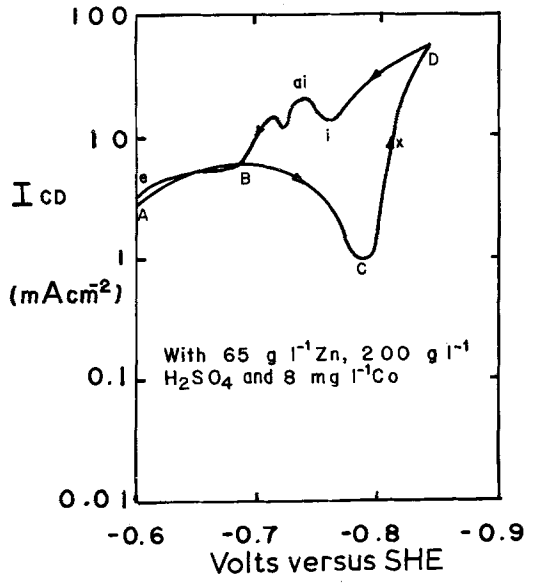

Fig. 3. Voltammogram obtained for electrolytes containing cobalt additions. $T = 45°$ C; scan rate = 0.5 mV s^{-1}.

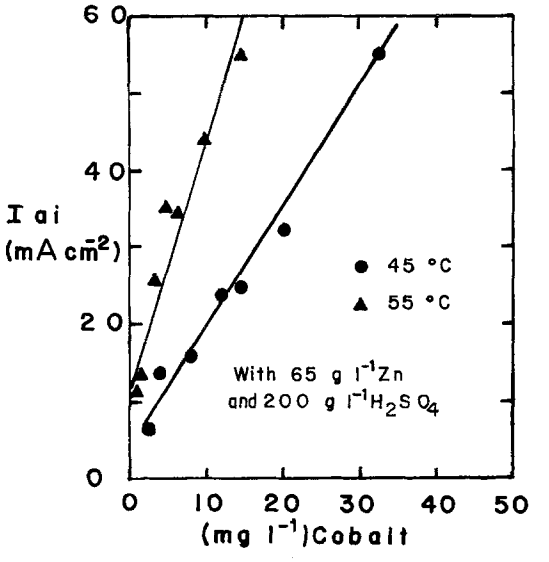

Fig. 5. Peak current density versus cobalt content. Scan rate = 0.5 mV s^{-1}.

temperature causes the peak height to increase at a given impurity concentration.

This peak appears only after some zinc has deposited. The peak does not appear when the cathodic sweep direction is reverse prior to reaching the zinc deposition potential. At this peak, vigorous hydrogen evolution occurs and the deposited zinc completely dissolves from the electrode surface even though the net current is cathodic. Stability tests conducted on electrolytes containing these impurities indicate that the zinc becomes completely unstable after the potential is made more positive than point i. At potential values more negative than point i, another phenomenon occurs for solutions containing moderate levels of impurity. Instead of reaching a constant current at a given potential, cycles of deposition and dissolution occur. Zinc deposits initially; but, with time, vigorous hydrogen evolution begins and very high current densities are obtained (200 mA cm^{-2}). The current peaks, then falls to relatively low values (< 10 mA cm^{-2}). The electrodes were checked for zinc on the SEM at this point, but neither zinc nor impurity metal were detected. Zinc redeposition begins after a certain time interval, and the sequence is repeated. The cycle time depends on the impurity concentation. Electrolysis studies done by other investigators confirm similar cyclic behaviour for solutions containing cobalt, nickel and germanium impurities [9, 10].

The impurities do not seem to accumulate on the working electrode. Continuous cycling yields relatively similar scans, which indicates little impurity accumulation. The impurities may become unstable when the zinc dissolves because of the loss in cathodic protection afforded by the presence of the deposited zinc or they may not adhere well to the aluminium substrate and are physically flushed from the electrode surface by the vigorous hydrogen evolution. If the impurities did accumulate on the electrode surface, higher hydrogen currents would be expected even after the zinc had completely dissolved because the exchange currents for hydrogen discharge on cobalt and germanium are significantly higher than that of aluminium or zinc and hydrogen discharge on these metals should be easier.

The point at which the zinc becomes completely unstable (point i) is found to occur at a potential value similar to that of the no-addition electrolyte (approximately -0.781 V versus SHE) and this point appears to depend only on the zinc and acid concentrations and not on the impurity concentration. Point i will be called the zinc instability potential in subsequent discussions.

Germanium and cobalt cause significant changes in the back scan, as demonstrated above, but do not affect the front scan. The zinc deposition potential and the potential at point x (potential which gives a current density of 10 mA cm^{-2}) are nearly identical. Deposit morphologies were also similar, as seen in Figs. 6 and 7. The deposits were obtained by scanning to point D and holding the potential constant at this point for 1 min. The coverage was evenly distributed for all these deposits and each crystallite appears to be growing independently of its neighbours. There appears to be little tendency for the particles to clump together. The crystallite size is quite similar for the deposits obtained from addition-free electrolytes and for those containing 0.1 mg l^{-1} germanium. The crystallite size is slightly smaller for the deposit obtained from the electrolyte containing 8 mg l^{-1} cobalt.

Since there is virtually no change in the front scan portion of the voltammogram, the amount of impurity deposition prior to zinc deposition appears to be insignificant or at least insufficient to cause any notable increase in the cathodic

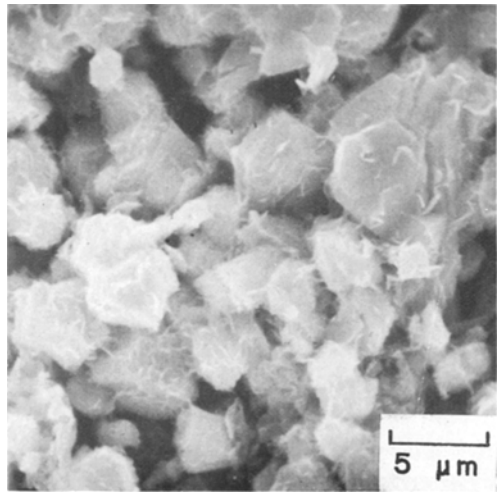

Fig. 6. Zinc deposit obtained for electrolyte containing 65 g l^{-1} Zn and 200 g l^{-1} H_2SO_4. Potential held at point D for 1 min (× 3000).

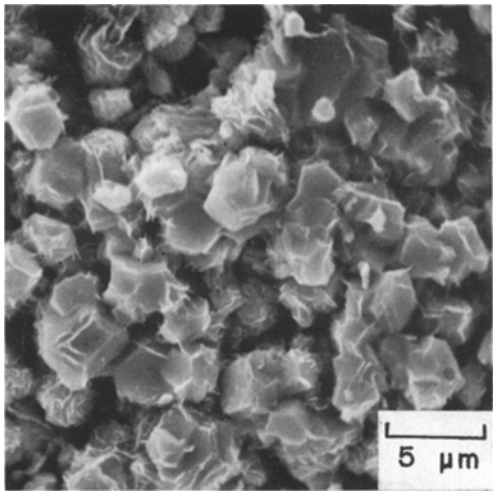

Fig. 7. Zinc deposit obtained for electrolyte containing 65 g l^{-1} Zn, 200 g l^{-1} H_2SO_4, and 8 mg l^{-1} Co. Potential held at point D for 1 min, (× 3000).

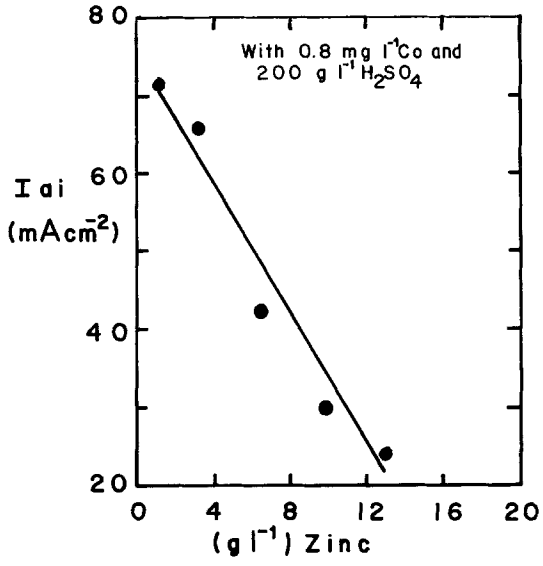

Fig. 8. Peak current density versus zinc concentration. Scan rate = 0.5 mV s^{-1}; T = 45° C.

hydrogen current. This is most likely due to the inhibiting effect of specifically absorbed zinc ions which greatly reduce the rate of discharge of the impurity ions. Other investigators have found that the presence of as little as 6 g l^{-1} Zn in a 1 M $CoSO_4$ electrolyte can prevent virtually any cobalt deposition at potentials less than the zinc discharge potential [21–23, 25, 26]. The retarding effect of the zinc ion is less when the zinc ions begin to deposit and significant amounts of impurity co-deposit with the zinc [23].

3.3. *Factors affecting the Co and Ge voltammograms*

It was found that increased temperature, surface roughness, acid concentration and decreased zinc concentration increase the peak current density at ai.

3.3.1. Zinc concentration. The effect of varying zinc concentration is shown in Fig. 8. Increasing the zinc concentration suppressed the effect of the impurity and also caused a shifting of the zinc deposition potential and zinc instability point to less negative potentials. Concentrations of 0.1 mg l^{-1} Co and 0.02 mg l^{-1} Ge could be detected by diluting the base electrolyte to 6.5 g l^{-1} Zn with 200 g l^{-1} sulphuric acid

3.3.2. Acid concentration. The interaction of the impurities was enhanced by increasing the sulphuric acid concentration. The cyclic voltammetry experiments indicate that significantly less impurity can be tolerated at higher acid concentrations, as might be expected. This is illustrated by the results shown in Fig. 9. Increasing acid concentration also increases the initial hydrogen ion reduction (see Fig. 10) during the cathodic sweep portion of the cycle. Increasing acid concen-

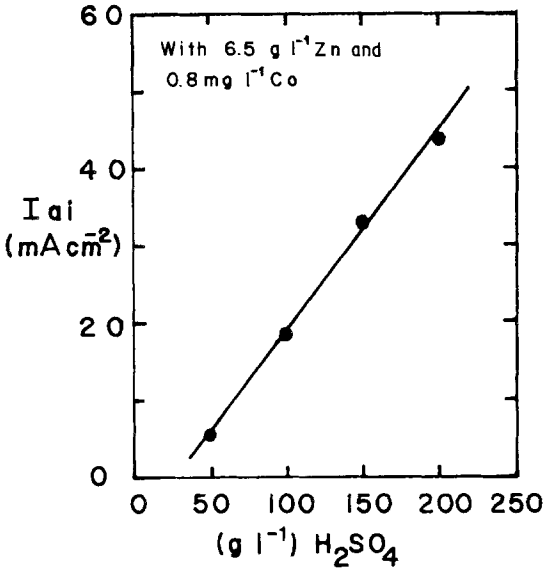

Fig. 9. Peak current density versus acid concentration. Scan rate = 0.5 mV s^{-1}; T = 45° C.

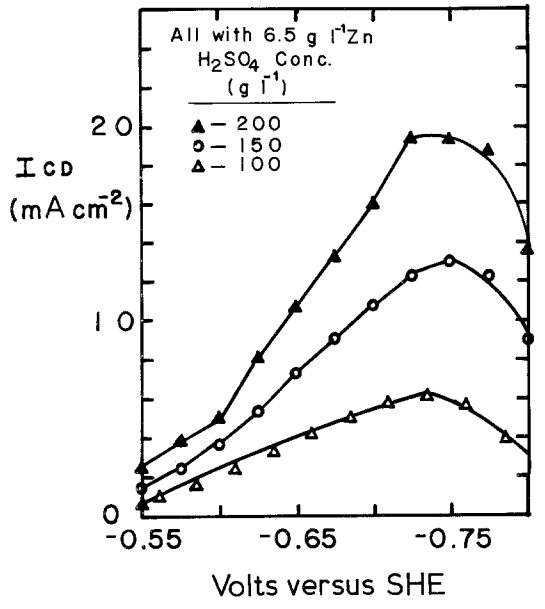

Fig. 10. Hydrogen current density versus electrode potential for electrolytes containing 6.5 g l^{-1} Zn and various H_2SO_4 concentrations. Scan rate = 0.5 mV s^{-1}; $T = 45°$ C.

trations lead to increased impurity effects and greater amounts of cathodically produced hydrogen. Both factors lead to a decrease in zinc current efficiency.

3.3.3. Surface roughness. The effect of increased surface roughness is illustrated by Fig. 11. The

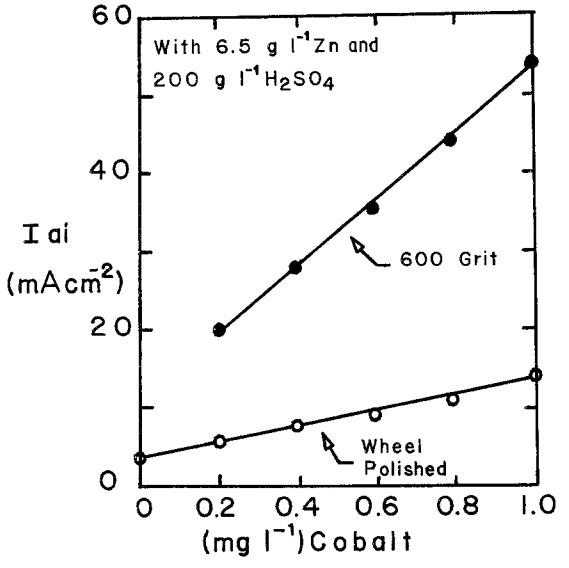

Fig. 11. Peak current density versus cobalt concentration for working electrodes having different surface preparation. Scan rate = 0.5 mV s^{-1}; $T = 45°$ C.

600 grit polished electrodes were more sensitive to increasing impurity content than the wheel-polished electrodes. Increasing surface roughness increases the detrimental interaction of the impurities at the electrode. The increased sensitivity of the rougher 600 grit polished electrodes was utilized by conducting most of the tests with these electrodes, but the variability was somewhat higher than that of the wheel-polished samples (± 3 mA cm^{-2} to ± 1 mA cm^{-2}).

3.3.4. Impurity concentration and temperature. The linearity of the peak current density with impurity concentration is illustrated by Figs. 12 and 13. Fig. 12 shows the results obtained for germanium and Fig. 13 for cobalt. The linear variation of peak current density with impurity concentration indicates indirectly that the rate of impurity deposition is diffusion controlled. Other investigators using different techniques have also found this to be the case for comparable impurity levels [11, 24, 27–29]. Fig. 13 also illustrates the effect of temperature on the peak current density. A temperature change from 35 to 55° C results in increased peak current densities for the same level of impurity concentration. The temperature increase also causes an enhanced impurity effect at the electrode and zinc stability is reduced. Higher temperatures increase the sensitivity of the cyclic voltammetry technique to the presence of impurities, allowing lower levels of detectability. For cobalt, the detectable limit is 0.4 mg l^{-1} at 35° C and 0.1 mg l^{-1} at 55° C for an

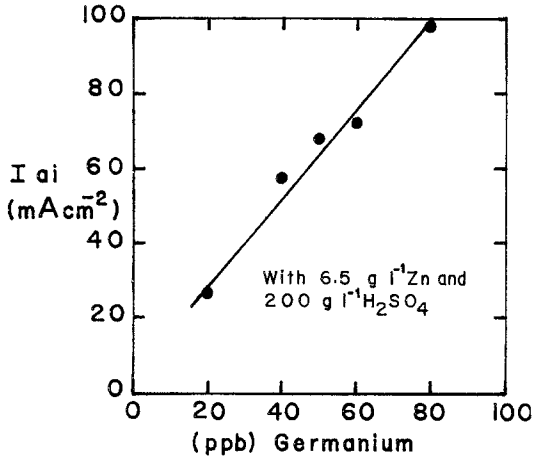

Fig. 12. Peak current density versus germanium concentration. Scan rate = 0.5 mV s^{-1}; $T = 45°$ C.

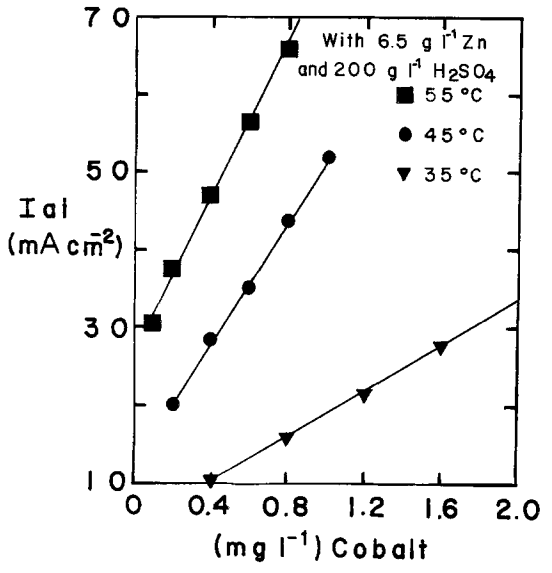

Fig. 13. Peak current density versus cobalt concentration for various temperatures. Scan rate = 0.5 mV s^{-1}.

electrolyte containing 6.5 g l^{-1} Zn and 200 g l^{-1} H_2SO_4.

3.3.5. *Test time.* The total test time of the voltammograms discussed thus far is approximately 25 min. This test time can be greatly reduced by using a fast scan speed for the front scan (5 mV s^{-1}) and a slow scan from point D on (0.5 mV s^{-1}). The resulting voltammogram is

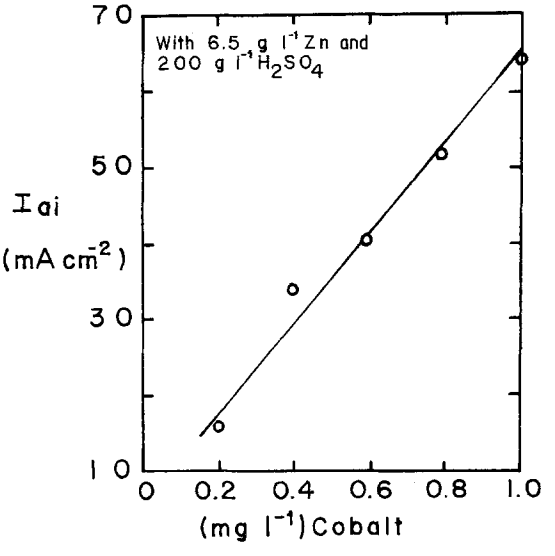

Fig. 14. Peak current density versus cobalt concentration. Fast scan (5 mV s^{-1}) to point D then slow scan (0.5 mV s^{-1}) back to starting potential.

similar in shape to that obtained using the slow scan throughout. The peak current densities again show the same type of relationship with impurity concentration (see Fig. 14). The reproducibility is not as good (± 4 mA cm^{-2}), but the total test time is reduced to 10 min.

Further work in this area is necessary to properly delineate the influence of the processing conditions on the voltammograms. However, the sensitivity and reproducibility of this technique are quite comparable to other common chemical analysis procedures now in use. An additional advantage is that the active impurity concentration present and not merely the physical quantity in solution is detected.

3.4. *Apparent mechanism of germanium and cobalt interaction at the working electrode*

The data obtained using the cyclic voltammetry technique indicate that germanium and cobalt behave similarly at the working electrode. The polarization behaviour in both cases is nearly the same. The main difference is that germanium interaction becomes apparent at lower concentration levels than for cobalt. For a solution containing 6.5 g l^{-1} Zn and 200 g l^{-1} H_2SO_4, a cobalt concentration of 0.4 mg l^{-1} was required to produce a peak current density of 28 mA cm^{-2}. A germanium concentration of 0.02 mg l^{-1} produced this same peak current density. This indicates that roughly 20 times the amount of cobalt as germanium is necessary to produce similar polarization behaviour.

The exchange current densities for hydrogen discharge on germanium, cobalt, and zinc are reported to be 1×10^{-5}, 4.5×10^{-7}, and 1.25×10^{-8} A cm^{-2}, respectively [24]. The higher exchange current densities for germanium and cobalt in comparison to zinc indicate that hydrogen discharge on these metals should be easier than on the zinc. It is interesting that the ratio of the exchange current values for germanium and cobalt is equal to 21. This ratio is nearly the same as that obtained for the ratio of cobalt to germanium needed to produce equivalent peak current densities. It appears that the interaction of the impurity is dependent on its ability to act as a site of hydrogen discharge. The degree of zinc corrosion and consequent loss in zinc

current efficiency depend on the concentration of impurity in the solution. The instability of the zinc, as shown by the cyclic behaviour of the zinc deposit in the presence of these impurities and the massive amounts of hydrogen that are liberated at the electrode as the zinc dissolves, seem to confirm a local cell type of impurity interaction. The cobalt and germanium sites act as local cathodes and the adjacent zinc sites as local anodes.

As the deposition process starts, both the impurities and the zinc are deposited over the whole electrode surface. The deposition rate of the impurity is proportional to its concentration in the electrolyte since the rate is diffusion-controlled. The surface remains generally smooth during the initial deposition period, and a uniform cathode potential exists without the presence of any extensive mixed potential regions. After a certain time, activation of the co-deposited impurities begins due to changes in the morphology or surface roughness. When the surface becomes rough, the specific cathode current density decreases at the recessed areas. A local potential difference is created, and zinc corrosion is initiated. As the zinc corrodes, more impurity is exposed, and it tends to agglomerate since it is cathodically protected. Hydrogen evolution increases because more sites favourable to hydrogen discharge are uncovered. The re-solution of the zinc proceeds at an ever increasing rate. The pH of the corrosion site can also be higher due to a deficiency in H^+ ions which are reduced to hydrogen. Thus, the potential differences between the corroding and non-corroding areas are accentuated, thereby increasing the driving force of the reaction. Once the process is initiated, it can sometimes become auto-catalytic.

The results of the cyclic tests support the above mechanism. Cycling of the zinc in the presence of the impurities; the formation of a peak current density; the massive amounts of hydrogen evolution that accompany zinc dissolution; and the favourable exchange current characteristic of germanium and cobalt all tend to confirm the proposed mechanism of impurity interaction.

4.4. *Summary*

Cyclic voltammetry techniques allow the determination of the effects of such factors as impurity concentration, zinc-to-acid ratio, temperature, and additives on zinc electrowinning solutions. These short-term tests for cobalt and germanium have proven to be correlatable with classical long-term efficiency tests in many instances [30].

The polarization behaviour of acid zinc sulphate electrolyte is shown to be very sensitive to the active species present. When the test parameters are varied, the changes in the scan curves can be used to evaluate the nature of the electrolyte. This provides a good method for both indicating the quality of the solution as well as giving a means for possible corrective actions if desired, without extensive current efficiency tests.

The mechanism responsible for reduced efficiencies from cobalt and germanium in zinc electrolysis appear to be similar. One logical model, based on the curves obtained, is the formation of local cells on the electrode surface. This enhances hydrogen reduction and zinc dissolution, which with time, causes the net cathode deposition process to deteriorate. The time and conditions required to initiate this zinc instability appear to be functions of the plating parameters, such as surface roughness, impurity concentration, acid to zinc ratio, and other chemical and electrochemical factors. It has often been assumed that germanium and antimony behave similarly. Comparisons of this study on germanium with previous research [1, 6] on antimony show substantial variations in polarization behaviour, and are indicative of differences in mechanistic aspects involved in zinc deposition processing efficiency.

Acknowledgements

The authors wish to acknowledge the financial assistance provided by the AMAX foundation, New York, N.Y. and by Bureau of Mines, US Department of Interior, Grant GO 264029. We would also like to acknowledge the technical assistance provided by Cominco Ltd, Trail, British Columbia, Canada. We also would like to thank Dr Yar-Ming Wang, formerly Assistant Research Professor at the University of Missouri-Rolla for his helpful advice and assistance concerning this study.

References

[1] D. R. Fosnacht and T. J. O'Keefe, paper presented at 107th Annual Meeting, A.I.M.E., Denver, Colorado (1978).
[2] D. J. MacKinnon and J. M. Brannen, *J. Appl. Electrochem.* 7 (1977) 451.
[3] D. J. Robinson and T. J. O'Keefe, *ibid* 6 (1976) 1.
[4] B. A. Lamping and T. J. O'Keefe, *Met. Trans. B* 7B (1976) 551.
[5] R. Liebscher, *Neue Heutte* 14 (1969) 651.
[6] R. C. Kerby, H. E. Jackson, T. J. O'Keefe and Y. Wang, *Met. Trans. B* 8B (1977) 661.
[7] D. R. Fosnacht, Masters Thesis, Columbia University, New York (1975).
[8] I. W. Wark, *Proceedings of the Australian Conference on Electrochemistry, 1st., Sydney, Hobart, Australia* (1963) pp. 889–900.
[9] M. Maja, *Electrochim. Metal.* 2 (1967) 469.
[10] M. Maja and S. Pozzoli, *Chim. Ind.* 51 (1969) 133.
[11] I. R. Bellobono, *Ind. Chem. Belge* 32 (1967) 305. 305.
[12] A. G. Pecherskaya and V. V. Stender, *J. Appl. Chem. USSR* 23 (1950) 975.
[13] U. F. Turomshina and V. V. Stender, *ibid* 27 (1954) 1019.
[14] G. Scacciati, *Industria mineraria* 4 (1953) 511.
[15] U. F. Turomshina and V. V. Stender, *J. Appl. Chem. USSR* 28 (1955) 447.
[16] G. Z. Kir'yakov, *Zhur. Fiz. Khim.* 32 (1958) 2561.
[17] A. F. Nikiforov, *J. Appl. Chem. USSR* 37 (1964) 360.
[18] Kurt Peukert and Willy Schreiter, *Metallurgie u. Gresserreitech* 4 (1954) 397.
[19] A. I. Levin, *et al*, *J. Appl. Chem. USSR* 31 (1958) 569.
[20] Y. Wang, T. J. O'Keefe and W. J. James, paper presented at 107th Annual Meeting, A.I.M.E., Denver, Colorado (1978).
[21] A. F. Nikiforov, *J. Appl. Chem. USSR* 37 (1964) 360.
[22] M. Yunus, C. Capel-Baute and C. Decroly, *Electrochim. Acta* 10 (1965) 885.
[23] B. P. Yur'ev, *Tr. Leningr. Politekhn. Inst.* 223 (1963) 87.
[24] G. C. Bratt, *Electrochem. Technol.* 2 (1964) 323.
[25] A. M. Ezrokhina and B. P. Yur'ev, *J. Appl. Chem. USSR* 42 (1969) 2697.
[26] A. M. Ezrokhina, *et al.*, *ibid* 45 (1972) 96.
[27] Niro Matsuura, *J. Chem. Soc. Japan, Pure Chem. Sect.* 74 (1953) 239.
[28] *Idem, Sci. Papers Coll. Gen. Educ. Univ. Tokyo* 3 (1953) 13.
[29] Z. A. Sheka, *Ukrain. Khim. Zhur.* 22 (1956) 394.
[30] D. R. Fosnacht, PhD Dissertation, University of Missouri-Rolla, Rolla, Missouri (1978).